COVER SHEET

Vibrational spectroscopy of the sorosilicate mineral hemimorphite $Zn_4(OH)_2Si_2O_7.H_2O$

Ray L. Frost•, Jocelyn M. Bouzaid, B. Jagannadha Reddy

Inorganic Materials Research Program, School of Physical and Chemical Sciences, Queensland University of Technology, GPO Box 2434, Brisbane Queensland 4001, Australia.

Abstract

Raman spectroscopy complimented by infrared spectroscopy has been used to study the mineral hemimorphite from different origins. The Raman spectra show consistantly similar spectra with only one sample showing additional bands due to the presence of smithsonite. Raman bands observed at 3510 to 3565 and 3436 to 3455 cm^{-1} are assigned to OH stretching vibrations. Using a Libowitzky type formula these OH bands provide hydrogen bond distances of 0.2910, 0.2825, 0.2762 and 0.2716 pm. Water bending modes are observed in the Raman spectrum at 1633 cm^{-1}. An intense Raman band at 930 cm^{-1} is attributed to SiO symmetric stretching vibration of the Si_2O_7 units. Raman bands observed at 451 and 400 cm^{-1} are attributed to out of plane bending vibrations of the Si_2O_7 units. Raman bands at 330, 280, 168 and 132 cm^{-1} are assigned to ZnO and OZnO vibrations.

Key words: hemimorphite, silicates, axinites, humites, Infrared and Raman spectroscopy

1. Introduction

Hemimorphite is a sorosilicate of formula $Zn_4Si_2O_7(OH)_2.H_2O$ [1, 2]. The nanme of the mineral comes from the term bipolar or *hemimorphic*. The termination of the crystal is different at each end of the crystal [3]. The crystal is is rather blunt being dominated by a pedion face while the opposite end, is terminated by the point of a pyramid [3]. The crystal structure contains tetrahedrons of ZnO_3 OH, interlocked with Si_2O_7 groups and water molecules. The zinc is at the center of the tetrahedron while the three oxygens, along with an OH group, are at the four points of the tetrahedron.The Mineral is orthorhombic with point group *mm*2. A molecular model of hemimorphite is shown in Figure 1. The mineral is formed from the breakdown of zinc minerals including sphalerite, smithsonite, hydrozincite, rosasite, aurichalcite and other zinc bearing minerals and is formed over oxidised, hydrothermal supergene deposits.

Hemimorphite was originally named calamine. However this name had been used for another mineral and hemimorphite was proposed. The *hemi* means half while the *morph* means shape and thus hemimorphite is aptly named. Only a few other minerals show hemimorphic character such as tourmaline, but none show it as well as hemimorphite. Clusters of hemimorphite that show well shaped crystals do not always

• Author to whom correspondence should be addressed (r.frost@qut.edu.au)

exhibit the hemimorphic character. Because the crystals of a single specimen tend to grow outward with either the upper or the "lower part of the crystal as the overall orientation for that specimen. In order to see the hemimorphic character either a doubly terminated specimen is necessary or two different clusters with different orientations may be observed. Specimens of hemimorphite tend to be of two very different forms. One form produces very glassy, clear or white, thin, bladed crystals, often well formed showing many crystal faces. Many times these crystals are arranged in fan shaped aggregates. The other form produces a blue to blue-green botryoidal crust that resembles

2. Experimental

2.1. Minerals

Selected hemimorphite minerals were obtained from the Mineral Research Company (http://www.minresco.com/default.htm) and other sources including Museum Victoria (Museum Victoria, Melbourne, Victoria, Australia). The samples were phase analysed by powder X-ray diffraction and for chemical composition by EDX measurements.

2.2. Raman microprobe spectroscopy

The crystals of hemimorphite were placed and oriented on the stage of an Olympus BHSM microscope, equipped with 10x and 50x objectives and part of a Renishaw 1000 Raman microscope system, which also includes a monochromator, a filter system and a Charge Coupled Device (CCD). Raman spectra were excited by a HeNe laser (633 nm) at a resolution of 2 cm^{-1} in the range between 100 and 4000 cm^{-1}. Repeated acquisition using the highest magnification was accumulated to improve the signal to noise ratio. Spectra were calibrated using the 520.5 cm^{-1} line of a silicon wafer. In order to ensure that the correct spectra are obtained, the incident excitation radiation was scrambled. Previous studies by the authors provide more details of the experimental technique. Spectra at liquid nitrogen temperature were obtained using a Linkam thermal stage (Scientific Instruments Ltd, Waterfield, Surrey, England). Details of the technique have been published by the authors [4-7].

2.3. Mid-IR spectroscopy

Infrared spectra were obtained using a Nicolet Nexus 870 FTIR spectrometer with a smart endurance single bounce diamond ATR cell. Spectra over the 4000–525 cm^{-1} range were obtained by the co-addition of 256 scans with a resolution of 4 cm^{-1} and a mirror velocity of 0.6329 cm/s. Spectra were co-added to improve the signal to noise ratio.

Spectral manipulation such as baseline adjustment, smoothing and normalisation were performed using the Spectracalc software package GRAMS (Galactic Industries Corporation, NH, USA). Band component analysis was undertaken using the Jandel 'Peakfit' software package which enabled the type of fitting function to be selected and allows specific parameters to be fixed or varied accordingly. Band fitting was done using a Lorentz-Gauss cross-product function with the minimum number of component bands used for the fitting process. The Lorentz -Gauss ratio was

maintained at values greater than 0.7 and fitting was undertaken until reproducible results were obtained with squared correlations of r^2 greater than 0.995.

3. Results and discussion

Factor Group Analysis

The classic rules of vibrational spectroscopy show that the free SiO_4^{4-} tetrahedron of T_d symmetry has a vibratonal set $\Gamma = 1A_1 + 1E + 1F_1 + 3F_2$. By eliminating translations and rotations the reduced repreentation $\Gamma' = 1A_1 + 1E + 2F_2$. Thus all in all four vibrations with the E vibration twice degenerate and the F vibration 3 times degenerate match up with the nine vibrations under the 3N-6 rule.

The linear $Si_2O_7^{6-}$ ion of assumed symmetry bar3_m has a vibration set $\Gamma_2 = 3A_{1g} + 1A_{1u} + 1A_{2g} + 4A_{2u} + 4E_g + 5E_u$ and without rotaions and translations $\Gamma'_2 = 3A_{1g} + 1A_{1u} + 1A_{2g} + 2A_{2u} + 3E_g + 4E_u$. So 14 vibrations with seven degenerate match up with the 21 vibrations under the 3N-6 rule. For the Si2o76- ion of mm2 binary symmetry ie with non-linear SiOSi bridges, the irrrducible represention $\Gamma_3 = 8A_1 + 5A_2 + 6B_2 + 8B_1$. This reduces to, upon elimination of the rotational and translational modes to $\Gamma_3 = 7A_1 + 4A_2 + 4B_2 + 6B_1$. Thus 21 predicted vibrations would be expected.

Raman Spectroscopy

The Raman spectra of hemimorphite from three different origins are shown in Figure 2. The results of the Raman and infrared spectroscopic analysis are reported in Table 1. Table 1 shows a comparison of the Raman spectroscopic data from three hemimorphite samples together with the infrared data from one sample. The table reports the peak postion (cm^{-1}), the relative intensity of the component bands as a percentage and the width of the bands (cm^{-1}).A very sharp band is observed in each of the three spectra at 930 cm^{-1}. This band is not symmetric. This means there are two component bands making up the spectral profile. This band may be band component analysed into two components at 931 and 926 cm^{-1}. The band width as full width at half peak maximum (FWHM) is 9.0 cm^{-1} for the first peak and between 13.7 and 15.0 cm^{-1} for the second peak. These bands are attributed to the SiO stretching vibration of the Si_2O_7 units. An intense band is observed at 1093 cm^{-1} for the white hemimorphite from Sardinia. This band is not observed in the Raman spectra of the other hemimorphite samples. It is interesting that Brunel and Verne reported a band in this position to the A_{1g} vibrational mode of the $Si_2O_7^{6-}$ units [8]. In the light of these Raman spectra this assignment is open to question. This band is ascribed to the symmetric stretching vibration of a carbonate impurity. Poulet and Mathieu assigned the band at 930 cm^{-1} to the A_1 mode of the $Si_2O_7^{6-}$ units [9]. No Raman spectra were reported in their article, only the results of the spectra. In the infrared spectrum of the hemimorphite from Arizona an intense band at 933 cm^{-1} is observed (Figure 2). Brunel and Vierne reported the infrared band at 932 cm^{-1} for a single crystal of hemimorphite and attributed the band to the B_1 vibrational mode [8]. These authors showed that the position of this band varied in position if the hemimorphite was powdered. Farmer ([10] page 296)showed there was a correlation between the wavenumber of the SiO antisymmetric stretching vibration and the SiO bond length

[10]. The ν_{as} vibration is localised on the bridging oxygen. Lazarev showed that this wavenumber is determined by the OSiO bond angle.

A band common to all three hemimorphite mineralsis the band at 674 cm^{-1}. Brunel and Vierne identified an infrared band in this position and assigned the band to an A1 vibration [8]. These workers showed that the position of this band varied according to the infrared tchniques used for measurement. In the infrared spectrum (Figure 3) an intense band is observed at 676 cm^{-1}. Poulet and Mathieu observed a Raman band in this position and an infrared band at 677 cm^{-1} of medium intensity [9]. The band position varied according to the experimental settings of the single crystal experiment. They assigned the band to a O-Si-O bending vibration [9]. The band observed at 729 cm^{-1} for the white hemimorphite sample is ascribed to a carbonate bending mode. The band is not observed in the Raman spectra of the other two hemimorphite samples. A low intensity band is observed in all of the Raman spectra at 556 cm^{-1}. A distinct infrared band of hemimorphite is observed at 597 cm^{-1} (Figure 3). Poulet and Mathieu observed a Raman band at 554 cm^{-1} in the Raman spectrum and at 545 cm^{-1} in the infrared spectrum [9]. Brunel and Vierne also defined a band at 563 cm^{-1} [8]. In this latetr work, the position of the band depended on the infrared technique used and upon the amount of sample in the KBr disc. This tends to suggest there was an interaction between the hemimorphite and the KBr. Such a problem is avoided by using reflectance techniques as reported in this research. In the spectrum of the brown hemimorphite sample a Raman band is obseved at 979 cm^{-1}. Such a band was observed by Poulet and Mathieu [9] and was attributed to A_2(ab) vibration. The band is also observed for the hemimorphite from Arizona but is of very low intensity.

A number of infrared bands are observed at 1078, 1049, 1043 and 1027 cm^{-1} (Figure 3). Poulet and Mathieu also observed infrared bands at 1380, 1170, 1085 and 1020 cm^{-1} and assigned these bands to δ OH vibrations. Brunel and Vierne also observed an infrared band at around 1090 cm^{-1}. However they attributed the band to E_u modes of the Si_2O_7 units. No Raman bands were observed in these positions which tends to suggest the assignment of Poulet and Mathieu is perhaps more accurate. A number of infrared bands are observed at 1386, 1357 and 1336 cm^{-1} (Figure 4). The probable assignemnt of these bands is to δ OH deformation modes.
The $\nu_{antisym}$ vibration is localised on the bridging oxygen. Lazarev showed that this wavenumber is determined by the OSiO bond angle. In the figure developed by Farmer, a band assigned to the antisymmetric stretching vibration at around 1110 cm^{-1} for pyromorphite is shown and is assigned to the SiO antisymmetric stretching vibration. Thus it is likely that the infrared bands observed by Poulet and Mathieu at 1170 and 1085 cm^{-1} are the infrared active Raman inactive antisymmetric stretching vibrations.

Two Raman bands are observed at 451 and 400 cm^{-1}(Figure 5) These bands are attributed to out of plane bending vibrations of the Si_2O_7 units. Poulet and mathieu also observed Raman bands in these positions and described the bands as "déformations angulaires et réseau" They also observed an infrared band at 450 cm^{-1}. bands in these positions are not able to be detected using the ATR technique with the diamond anvil cell as the cell absorbs at wavenumbers below 550 cm^{-1}. An intense Raman band is observed at 330 cm^{-1}. This band is attributed to the Zn-O stretching vibration. A second band is observed at around 280 cm^{-1}. This band may also be

assigned to a ZnO stretching vibration. The band at 303 cm^{-1} for the white hemimorphite from Sardinia is considered to be due to a ZnO stretching vibration of the zinc carbonate impurity. The intense bands at 168 and 132 cm^{-1} are ascribed to the OZnO bending vibrations.

In the Raman spectra bands of significant intensity are observed around 1634 cm^{-1} (Figure 6). In the infrared spectrum (Figure 4) a distinct band is observed at 1633 cm^{-1}. These bands are attributed to δ H_2O vibrations. In some ways it is unusual to observed the water bending mode in the Raman spectrum. The band is normally intense in the infrared spectrum and is of very low intensity or is not al all observed in the Raman spectrum. These results compare well with those of Brunel and Vierne and also Poulet and Mathieu [8, 9]. Both previous studies showed the infrared bands of water in hemimorphite. In the structure of hemimorphite, perpendicular to the *C* axis, four, siz and eight fold tetyrahedral rings are formed. The six and eight fold rinmgs are connected along the *C* axis in wide channels which are occupied by water molecules. It is these water molecules which give the deformation modes at 1630 cm^{-1}. These water molecules must be in an ordered arrangement to give a water bending mode in the Raman spectrum of significant intensity.

The Raman spectra of hemimorphite from three different loacalities show consistantly similar spectra, especially in the OH stretching region (Figure 7). Two Raman bands are observed at around 3510 to 3565 and 3436 to 3455 cm^{-1}. These bands are assigned to OH stretching vibrations of the mineral $Zn_4Si_2O_7(OH)_2.H_2O$. Raman bands are observed at around 3328 and 3240 cm^{-1} and are attributed to the OH stretching vibrations of the OH units. Polarized FTIR absorption spectra of oriented hemimorphite crystals have been published [11, 12]. Infrared spectra of the Aizona hemimorphite in the OH stretching region are shown in Figure 8.

Studies have shown a strong correlation between OH stretching frequencies and both O···O bond distances and H···O hydrogen bond distances [13-16]. Libowitzky (1999) showed that a regression function can be employed relating the hydroxyl stretching frequencies with regression coefficients better than 0.96 using infrared spectroscopy [17]. The function is described as: $\nu_1 = (3592 - 304) \times 109^{\frac{-d(O-O)}{0.1321}}$ cm^{-1}. Thus OH---O hydrogen bond distances may be calculated using the Libowitzky empirical function. The values for the OH stretching vibrations listed above provide hydrogen bond distances of 3510 cm^{-1} gives a calculated hydrogen bond distance of 0.2910 pm, 3436 cm^{-1} → 0.2825 pm, 3739 cm^{-1} → 0.2762 pm and 3235 cm^{-1} → 0.2716 pm. The conclusion may be drawn that the hydrogen bond distances formed from the water units are stronger than those formed from the OH units.

4. Conclusions

Hemimorphite because of its nature is mots interesting to study using vibrational spectroscopic techniques. In this paper we report the study of hemimorphite minerals from three different origins and show that a carbonate

impurity is found in some of the mineral samples. Raman bands observed at 3510 to 3565 and 3436 to 3455 cm^{-1} are assigned to OH stretching vibrations. Using a Libowitzky type formula these OH bands provide hydrogen bond distances of 2.910, 2.825, 2.762 and 2.716 Å. Water bending modes are observed in the Raman spectrum at 1633 cm^{-1}. An intense Raman band at 930 cm^{-1} is attributed to SiO symmetric stretching vibration of the Si_2O_7 units.

Acknowledgments

The financial and infra-structure support of the Queensland University of Technology, Inorganic Materials Research Program is gratefully acknowledged. The Australian Research Council (ARC) is thanked for funding the instrumentation. Mr D. A. Henry of Museum Victoria (Melbourne, Australia) is thanked for the loan of the mineral samples.

References

1. Liu, Y., J. Deng, Q.-f. Wang, and Y.-h. Zhou, *Crystal chemistry and color genesis of the hemimorphite from Jinding Pb-Zn deposit, Yunnan Province.* Gaoxiao Dizhi Xuebao, 2005. **11**(3): p. 434-441.
2. Nakamura, R., K. Arikata, Y. Suginohara, and T. Yanagase, *Structure of silicates as studies by trimethylsilylation.* Kogaku Shuho - Kyushu Daigaku, 1977. **50**(5): p. 635-41.
3. Anthony, J.W., R.A. Bideaux, K.W. Bladh, and M.C. Nichols, *Handbook of Mineralogy*. Silica, silicates. Vol. 2 (part 1). 1995, Tuscon, Arizona, USA: Mineral Data Publishing.
4. Frost, R.L., D.A. Henry, and K. Erickson, *Raman spectroscopic detection of wyartite in the presence of rabejacite.* Journal of Raman Spectroscopy, 2004. **35**(4): p. 255-260.
5. Frost, R.L., *An infrared and Raman spectroscopic study of the uranyl micas.* Spectrochimica Acta, Part A: Molecular and Biomolecular Spectroscopy, 2004. **60A**(7): p. 1469-1480.
6. Frost, R.L., O. Carmody, K.L. Erickson, M.L. Weier, and J. Cejka, *Molecular structure of the uranyl mineral andersonite-a Raman spectroscopic study.* Journal of Molecular Structure, 2004. **703**(1-3): p. 47-54.
7. Frost, R.L., O. Carmody, K.L. Erickson, M.L. Weier, D.O. Henry, and J. Cejka, *Molecular structure of the uranyl mineral uranopilite-a Raman spectroscopic study.* Journal of Molecular Structure, 2004. **733**(1-3): p. 203-210.
8. Brunel, R. and R. Vierne, *Vibration spectra of hemimorphite.* Bulletin de la Societe Francaise de Mineralogie et de Cristallographie, 1977. **100**(1): p. 14-20.
9. Poulet, H. and J.P. Mathieu, *Vibration spectra and structure of hemimorphite.* Bulletin de la Societe Francaise de Mineralogie et de Cristallographie, 1975. **98**(1): p. 3-5.
10. Farmer, V.C., *Mineralogical Society Monograph 4: The Infrared Spectra of Minerals*. 1974. 539 pp.
11. Libowitzky, E., T. Kohler, T. Armbruster, and G.R. Rossman, *Proton disorder in dehydrated hemimorphite. IR spectroscopy and x-ray structure refinement at low and ambient temperatures.* European Journal of Mineralogy, 1997. **9**(4): p. 803-810.
12. Libowitzky, E. and G.R. Rossman, *IR spectroscopy of hemimorphite between 82 and 373 K and optical evidence for a low-temperature phase transition.* European Journal of Mineralogy, 1997. **9**(4): p. 793-802.
13. Emsley, J., *Very strong hydrogen bonding.* Chemical Society Reviews, 1980. **9**: p. 91-124.
14. Lutz, H., *Hydroxide ions in condensed materials - correlation of spectroscopic and structural data.* Structure and Bonding (Berlin, Germany), 1995. **82**: p. 85-103.
15. Mikenda, W., *Stretching frequency versus bond distance correlation of O-D(H)...Y (Y = N, O, S, Se, Cl, Br, I) hydrogen bonds in solid hydrates.* Journal of Molecular Structure, 1986. **147**: p. 1-15.
16. Novak, A., *Hydrogen bonding in solids. Correlation of spectroscopic and crystallographic data.* Structure and Bonding (Berlin), 1974. **18**: p. 177-216.

17. Libowitsky, E., *Correlation of the O-H stretching ferequencies and the O-H...H hydrogen bond lengths in minerals.* Monatschefte fÜr chemie, 1999. **130**: p. 1047-1049.

List of Figures

Figure 1 Model of hemimorphite structure

Figure 2 Raman spectra of hemimorphite in the 500 to 1200 cm^{-1} range.

Figure 3 Infrared spectra of hemimorphite in the 550 to 1150 cm^{-1} range.

Figure 4 Infrared spectra of hemimorphite in the 1250 to 1650 cm^{-1} range.

Figure 5 Raman spectra of hemimorphite in the 100 to 500 cm^{-1} range.

Figure 6 Raman spectra of hemimorphite in the 1200 to 1800 cm^{-1} range.

Figure 7 Raman spectra of hemimorphite in the 3125 to 3725 cm^{-1} range.

Figure 8 Infrared spectra of hemimorphite in the 2750 to 3750 cm^{-1} range.

List of Tables

Table 1 Table of the results of the Raman and infrared spectroscopic analysis of hemimorphite

Table 1 Table of the results of the Raman and infrared spectroscopic analysis of hemimorphite

Hemimorphite-white (Sardinia, Italy)			Hemimorphite-brown (Sardinia, Italy)			Hemimorphite (Arizona, USA)					
Raman			Raman			Raman			Infrared		
Centre cm^{-1}	FWHM cm^{-1}	% Area	Centre cm^{-1}	FWHM cm^{-1}	% Area	Centre cm^{-1}	FWHM cm^{-1}	% Area	Centre cm^{-1}	FWHM cm^{-1}	% Area
						3565	120.5	4.65	3352	218.4	18.37
3534	157.0	11.92							3297	48.1	1.33
			3510	165.3	10.52				3234	59.6	4.94
						3455	171.3	42.75	3180	236.1	9.64
3438	130.0	15.33	3436	125.8	24.23						
			3339	121.4	6.10						
3328	98.5	6.22				3321	74.8	1.59			
3240	111.2	6.36	3235	99.8	3.56	3240	116.0	4.83			
1733	10.5	0.32									
1634	12.1	0.36	1634	12.2	0.40	1634	16.5	0.40	1633	15.6	0.25
									1588	10.8	0.14
									1548	17.4	0.57
									1514	36.7	4.86
1406	6.9	0.99							1496	43.5	11.77
			1366	27.9	0.18	1366	29.6	0.21	1386	39.6	6.29
									1357	26.9	1.61
									1336	66.9	2.46
									1335	16.5	0.60
1196	40.4	0.53	1195	50.1	0.59				1105	47.7	1.05
									1078	39.4	2.90
									1049	9.9	0.38
1093	6.4	3.56				1180	114.9	1.17	1043	15.4	0.52
1090	9.0	5.38	1084	89.7	0.86				1027	39.3	2.26
						996	45.8	0.50			
			979	25.4	1.77				974	61.7	4.89

931	9.0	5.97	931	9.0	6.47	930	9.2	6.34	933	57.3	7.69
926	14.1	14.42	926	13.7	12.44	926	15.0	12.28	894	48.4	3.40
			861	10.4	0.07				863	18.9	0.96
									836	19.1	4.28
									831	117.2	4.74
									737	17.6	0.82
729	5.9	0.45							709	8.5	0.66
674	13.6	1.91	674	13.7	3.33	674	14.2	1.69	702	15.5	0.42
									676	27.6	1.29
									609	13.8	0.39
565	23.2	0.27	556	11.8	0.32	555	11.5	0.62	597	17.2	0.52
554	9.4	0.25									
451	12.5	4.63	451	13.9	5.97	451	12.8	3.31			
400	29.7	1.77	400	41.5	5.17	399	34.6	4.42			
329	9.3	1.48	330	10.0	2.46	330	9.8	1.91			
303	12.2	2.85									
275	19.4	0.71	282	20.1	1.33	274	19.9	0.72			
			266	22.0	0.87						
			231	51.1	2.65	230	53.3	0.69			
212	24.8	0.93	211	21.1	1.87	213	17.5	0.67			
194	9.7	1.44	194	16.9	0.34	193	11.9	0.59			
168	13.6	3.95	167	14.4	1.58	168	12.0	3.19			
152	39.2	2.29				157	34.8	2.40			
			142	35.1	3.02						
132	13.0	4.92	132	11.8	3.57	132	14.2	4.44			
111	12.5	0.77	110	13.1	0.35	111	14.8	0.61			

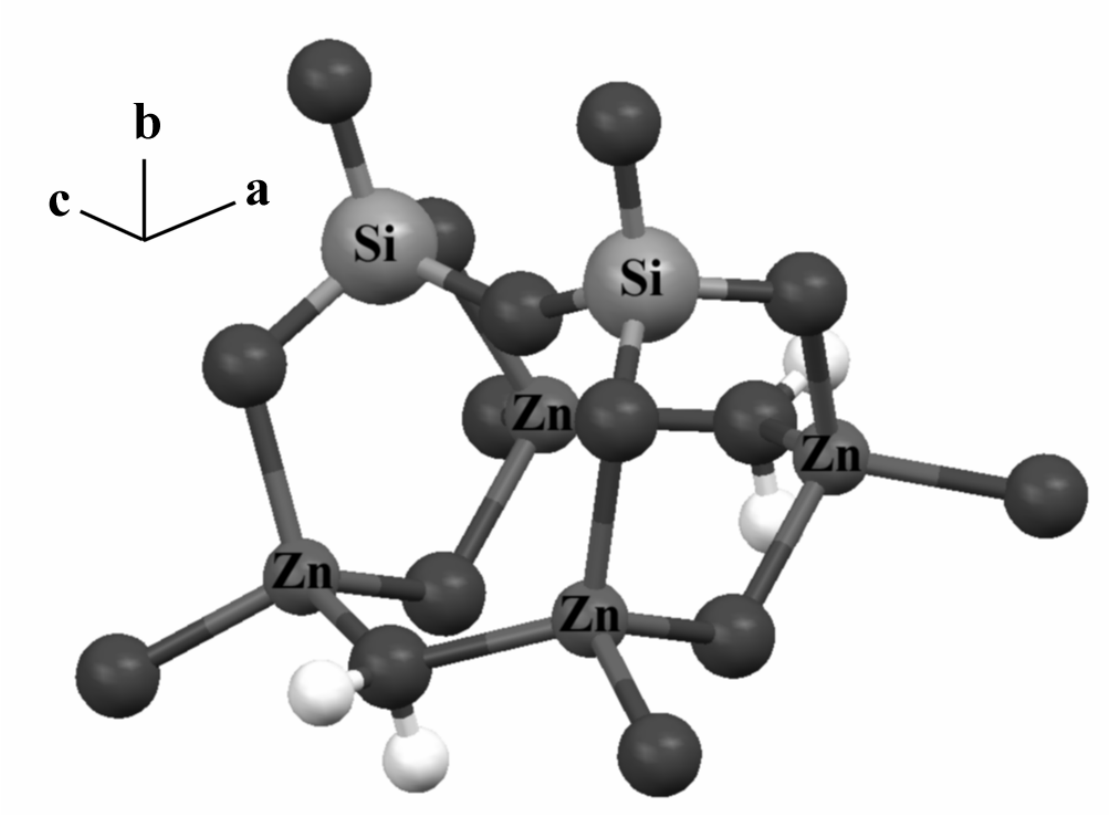

Figure 1 Model of hemimorphite structure

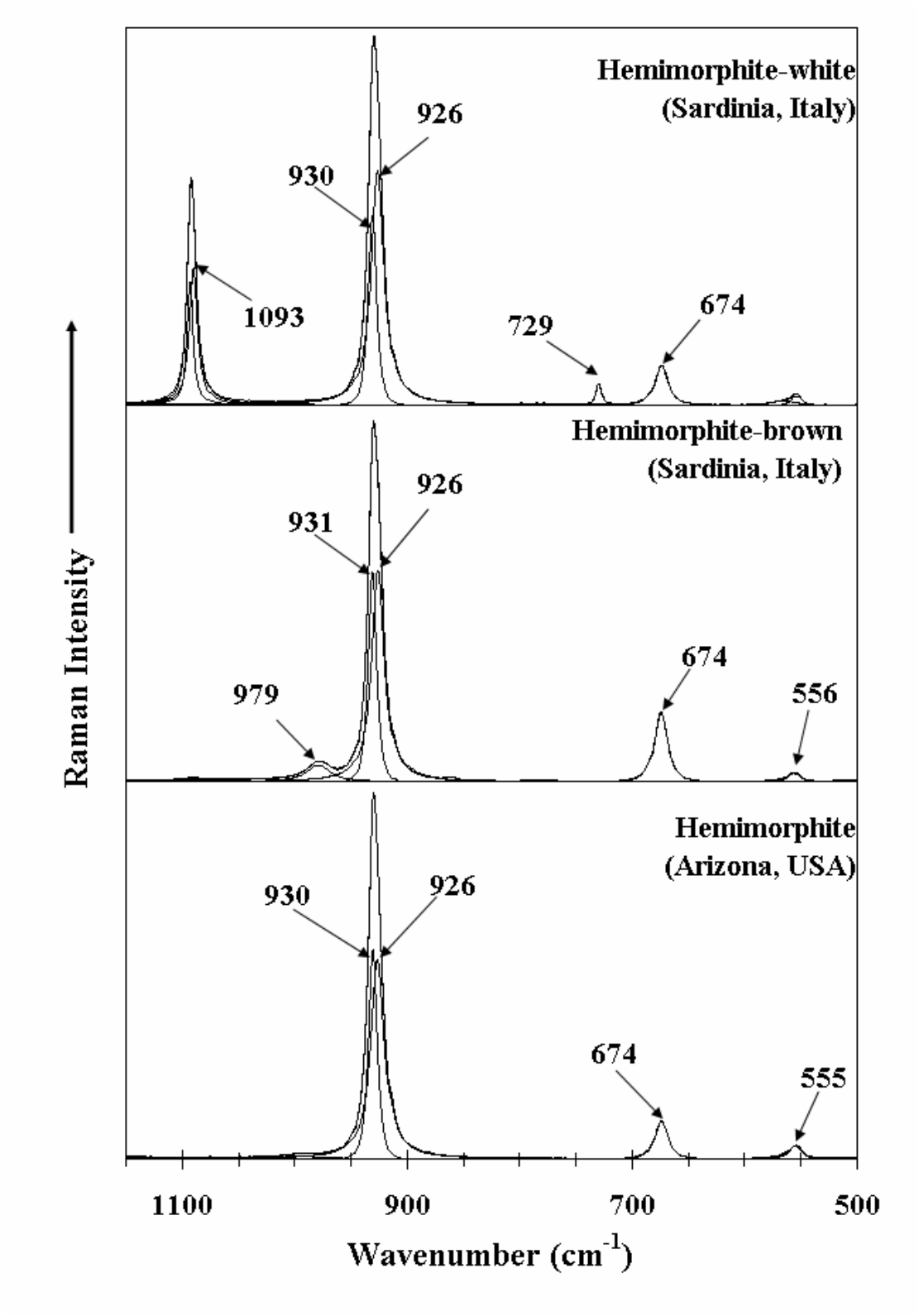
Hemimorphite-white
(Sardinia, Italy)
926
930
1093
729
674
Hemimorphite-brown
(Sardinia, Italy)
926
931
979
674
556
Hemimorphite
(Arizona, USA)
930
926
674
555
Raman Intensity
1100
900
700
500
Wavenumber (cm-1)

Figure 2

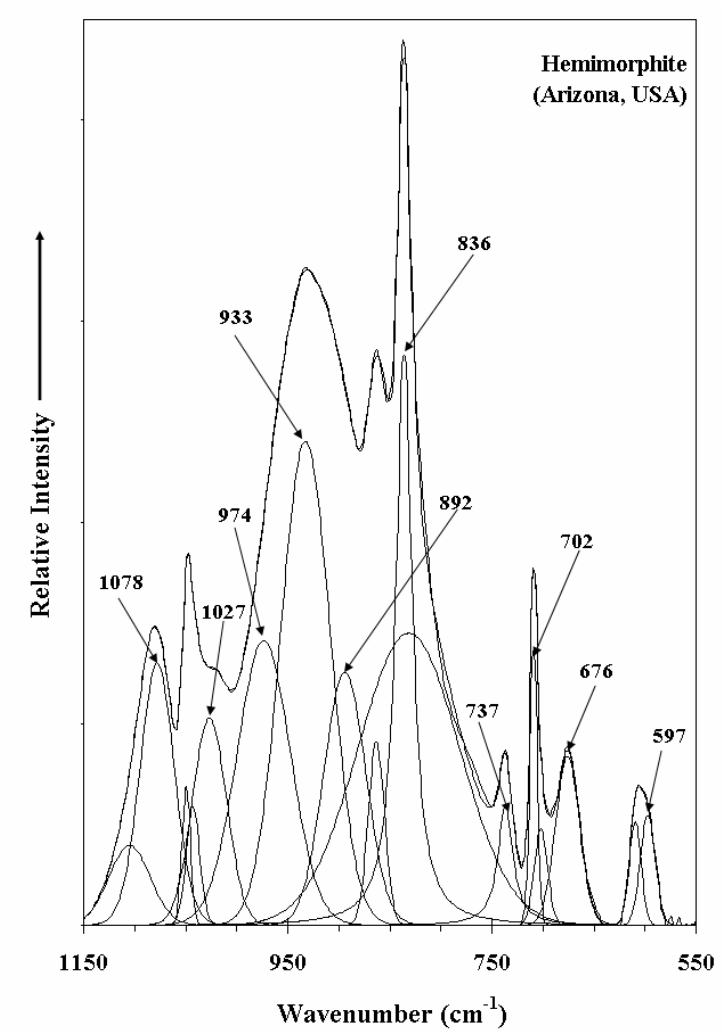
Hemimorphite
(Arizona, USA)
Relative Intensity
836
933
892
974
702
1078
1027
676
737
597
1150
950
750
550
Wavenumber (cm-1)

Figure 3

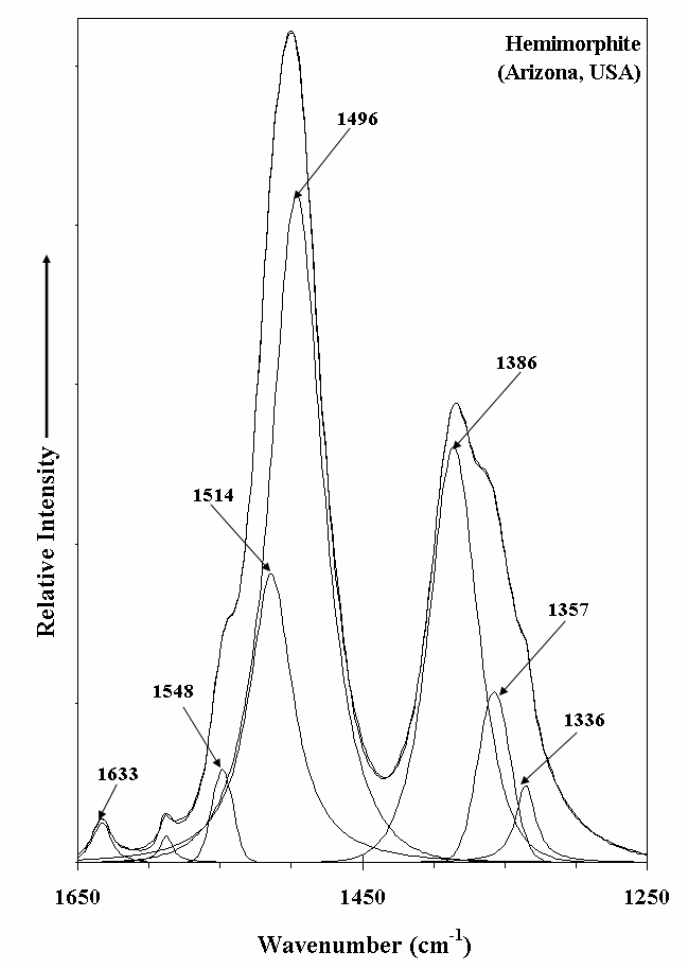
Hemimorphite
(Arizona, USA)
1496
1386
1514
1357
1548
1336
1633
Relative Intensity
1650
1450
1250
Wavenumber (cm-1)

Figure 4

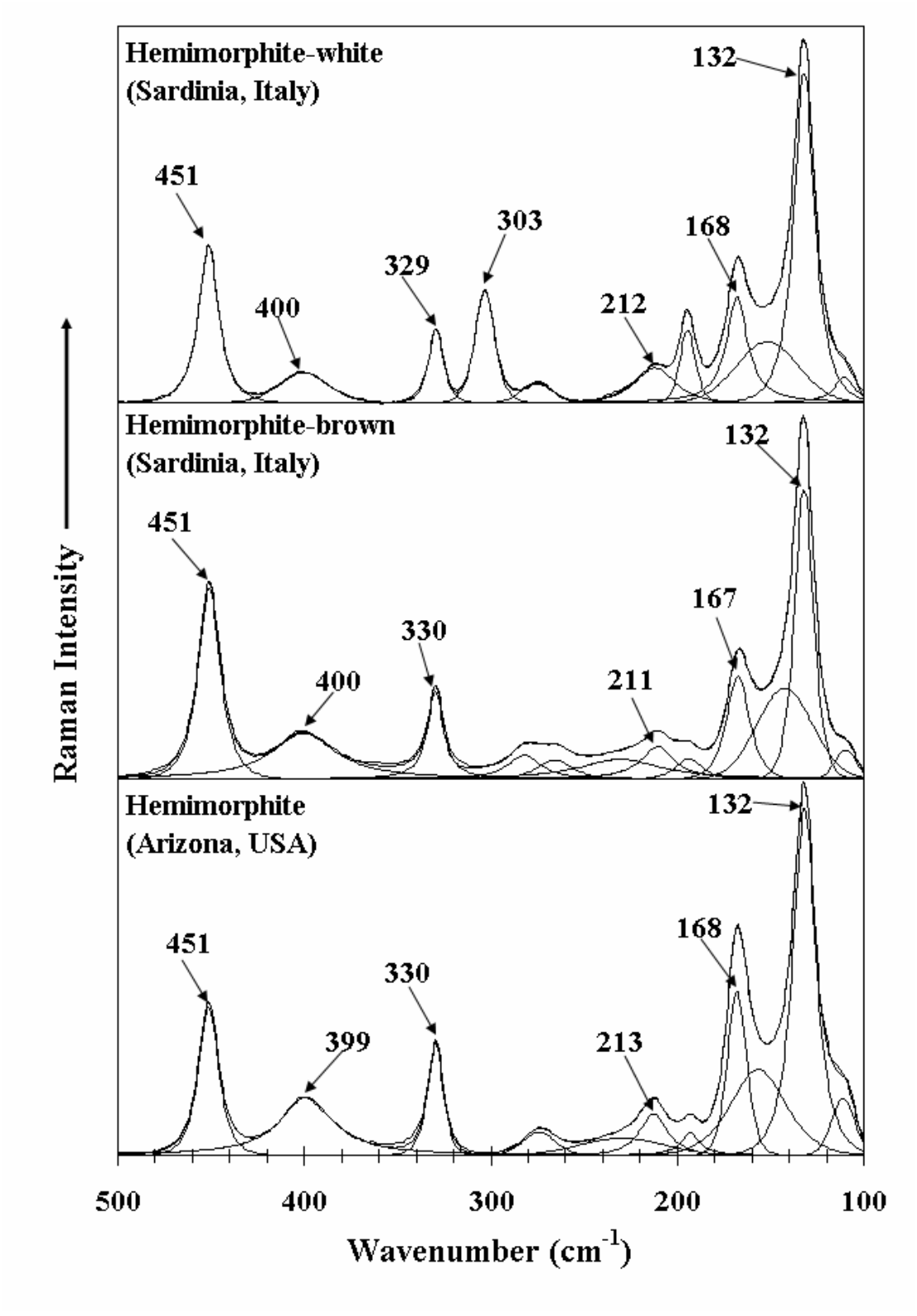
Hemimorphite-white
(Sardinia, Italy)
132
451
303
168
329
400
212
Hemimorphite-brown
(Sardinia, Italy)
132
451
167
330
400
211
Hemimorphite
(Arizona, USA)
132
168
451
330
399
213
Raman Intensity
500
400
300
200
100
Wavenumber (cm-1)

Figure 5

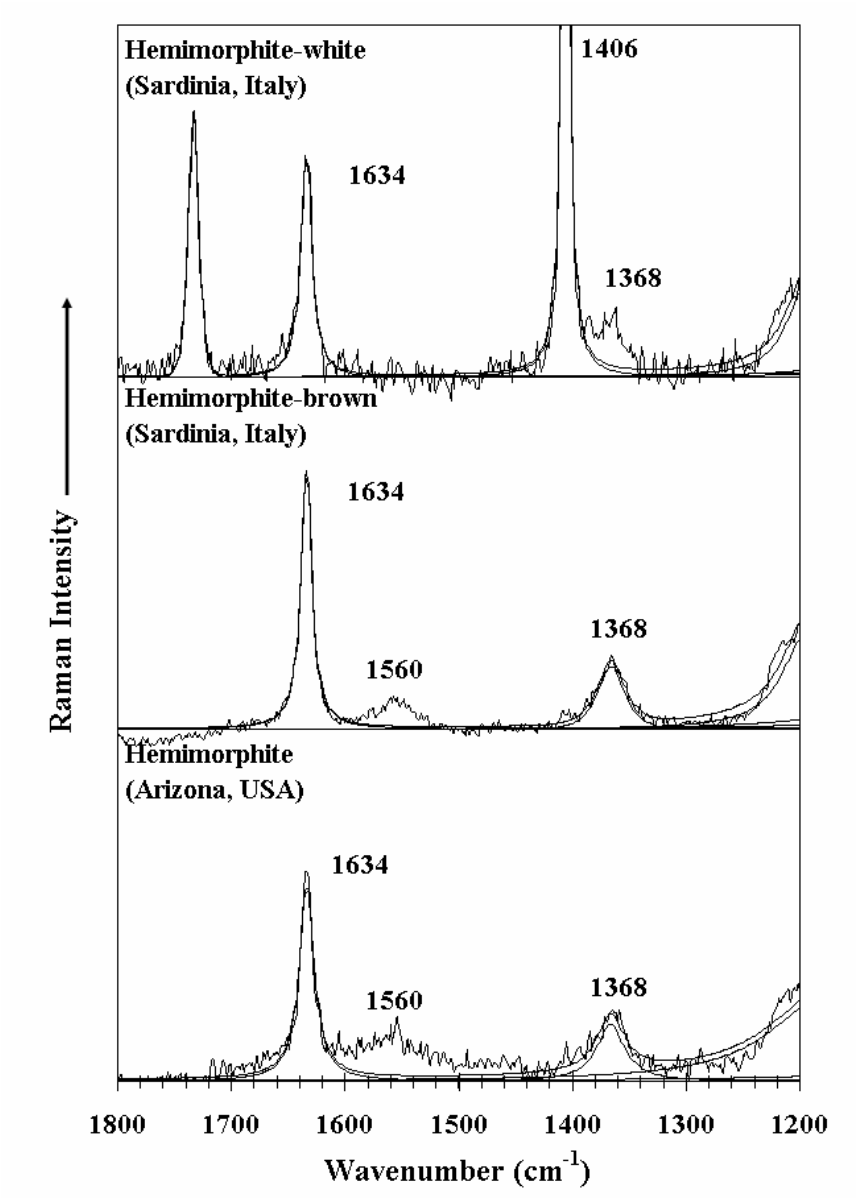
Hemimorphite-white
(Sardinia, Italy)
1406
1634
1368
Hemimorphite-brown
(Sardinia, Italy)
1634
1368
1560
Hemimorphite
(Arizona, USA)
1634
1560
1368
Raman Intensity
1800
1700
1600
1500
1400
1300
1200
Wavenumber (cm-1)

Figure 6

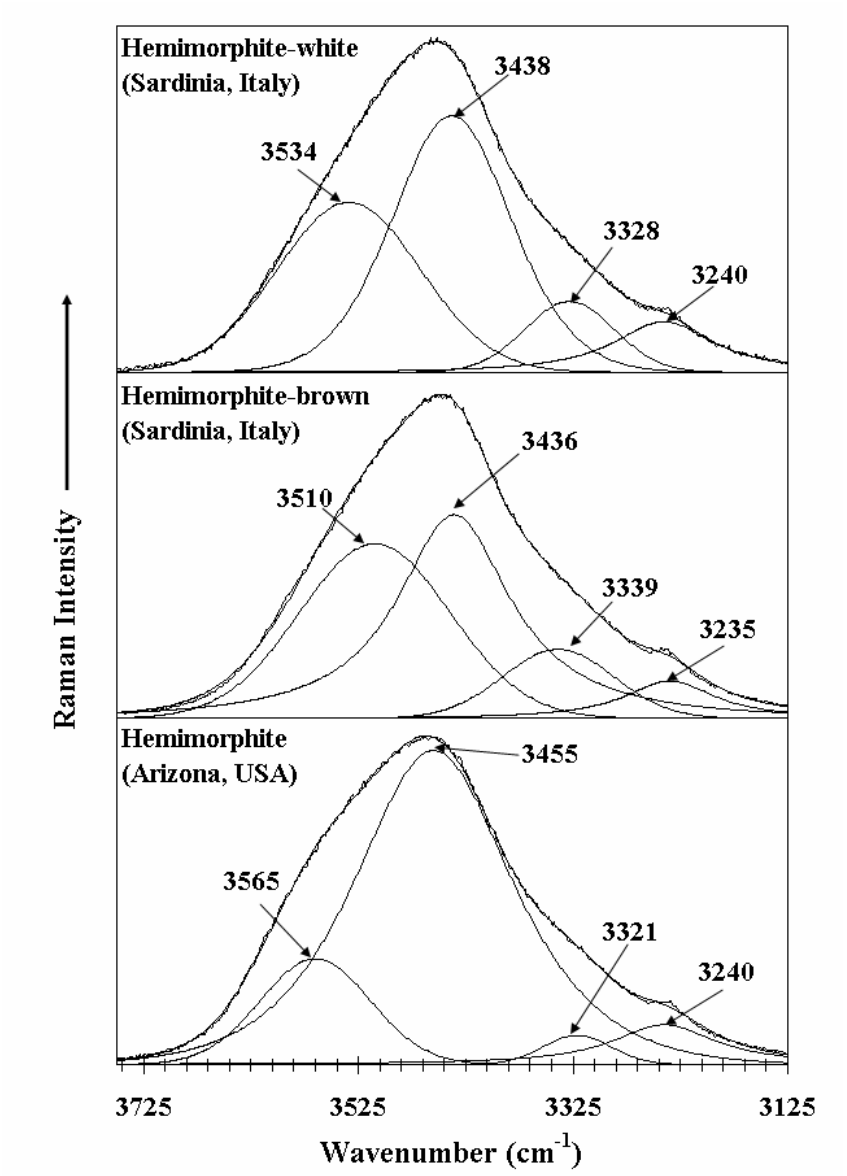
Hemimorphite-white
(Sardinia, Italy)
3438
3534
3328
3240
Hemimorphite-brown
(Sardinia, Italy)
3436
3510
3339
3235
Hemimorphite
(Arizona, USA)
3455
3565
3321
3240
Raman Intensity
3725
3525
3325
3125
Wavenumber (cm-1)

Figure 7

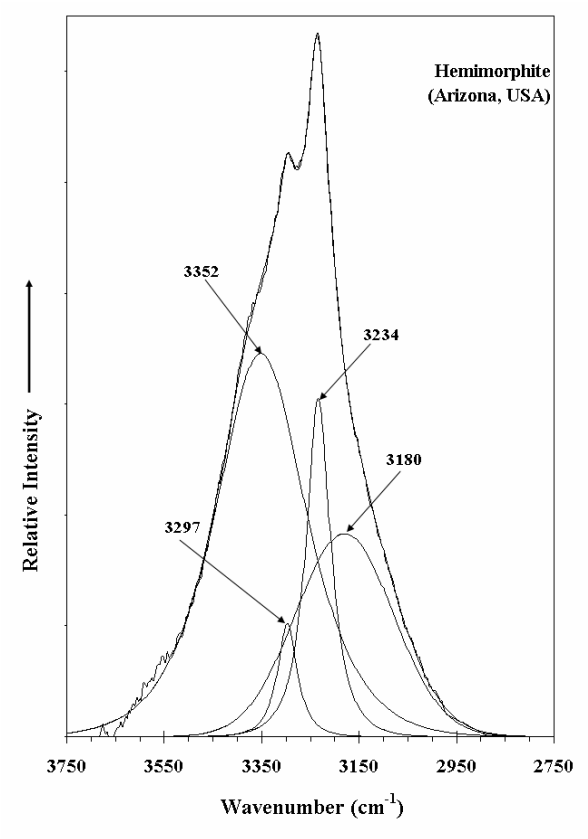
Hemimorphite
(Arizona, USA)
3352
3234
3180
3297
Relative Intensity
3750
3550
3350
3150
2950
2750
Wavenumber (cm-1)

Figure 8